Electrochemical determination of neurotransmitter serotonin using boron/nitrogen co-doped diamond-graphene nanowall-structured particles

Suchanat Boonkaew [a,*], Anna Dettlaff [b], Michał Sobaszek [c], Robert Bogdanowicz [c], Martin Jönsson-Niedziółka [a,*]

[a] Institute of Physical Chemistry, Polish Academy of Sciences, 44/52 Kasprzaka, Warsaw 01-224, Poland
[b] Department of Energy Conversion and Storage, Faculty of Chemistry, Gdańsk University of Technology, 11/12 Gabriela Narutowicza, Gdańsk 80-233, Poland
[c] Department of Metrology and Optoelectronics, Faculty of Electronics, Telecommunications and Informatics, Gdańsk University of Technology, 11/12 Gabriela Narutowicza, Gdańsk 80-233, Poland

ARTICLE INFO

ABSTRACT

Electrode fouling is a major issue in biological detection due to the adhesion of the protein itself and polymerization of biomolecules on the electrode surface, impeding the electron transfer ability and decreasing the current response. To overcome this issue, the use of anti-fouling material, especially boron-doped diamond (BDD) electrode, is an alternative way. However, the electrocatalytic activity of BDD is inadequate compared with graphene nanowalls, or other sp^2 phase materials. Furthermore, the contamination from other metals during the synthesis of BDD can affect the electrochemical analysis. Herein, for the first time, we report boron/nitrogen co-doped with diamond graphene nanowalls (DGNW) integrated with the screen-printed graphene electrode (SPGE) for the detection of serotonin (5-HT) as a model system. DGNW shows the integration of sp^2 and sp^3 hybridized phases, leading to a high surface area, high electrocatalytic activity, wide potential window, and a low background current. DGNWs prepared under different conditions were investigated and characterized. Compared to the bare SPGEs, the DGNW modified electrode exhibited good electrochemical performance and a superior anti-fouling ability for neurotransmitter detection. A significant enhancement in current response in a concentration-dependent manner was obtained using differential pulse voltammetry (DPV) in the presence of 5-HT from 1 to 500 μM ($R^2 > 0.99$) with a low detection limit (0.28 μM). Moreover, this proposed method was applied in a synthetic urine sample to confirm its biological applicability. These results show that the DGNW modified electrode could be productively utilized as an alternative electrochemical transducer with a good anti-fouling performance.

1. Introduction

Carbon-based nanomaterials have been attractive interest as electrode materials over the past few decades, particularly in electrochemical sensors, biosensors, and bioelectronics [1,2]. Carbon-based electrodes, including graphene [3], glassy carbon [1,4], carbon nanotubes (CNTs) [5–7], multiwall carbon nanotubes (MWCNT) [8], and carbon nanowalls (CNWs) [9] are one of the most attractive materials for electrochemical sensing applications due to their remarkable electrochemical properties. These materials are formed in sp^2-bonded carbon, leading to high electrical conductivity and good electrocatalytic activity for a variety of redox reactions [2,10]. Nonetheless, sp^2 carbon electrodes are prone to surface fouling, which negatively impacts on target analyte adsorption, electrical conductivity, and electrocatalysis, resulting in poor limit of detection (LOD) and reduced

device lifetime [11]. Moreover, a high background current and narrow electrochemical potential window of sp^2-bonded carbon have limited the application and functionalities of the electrodes. Therefore, diamond [12] and another hybridized phase called "sp^3-bonded diamond materials" have gathered increasing attention.

Since pure diamond is an insulator, its use as electrode material requires a controlled introduction of impurities called dopants. As a result, doped diamond achieves metal-like conductivity [13]. The most commonly used diamond dopant is boron which possesses one fewer electron than carbon; thus, boron-doped diamond (BDD) is p-type material (sp^3-diamond phase). BDD electrodes have been reported as detection electrodes for electrochemical sensors with different applications such as heavy metal [14], food and pharmaceutical controls [15], neurotransmitters [16], biomolecules, and biomarkers [17,18]. These electrodes are highly demanded features such as wide working poten-

tial window, chemical resistance, anti-fouling properties, and biocompatibility, thus enabling them to be reused several times without a decrease in current responses [14,18]. Due to BDD surfaces having a lower amount of surface functional groups or the lack of oxygen functional group on the diamond surface compared to conventional carbon-based materials, indicating that a very low tendency for adsorption of chemical species, proteins, and biomolecules on the inert diamond surface [19,20]. Even though the BDD electrode has been widely used in various electrochemical applications, the electrocatalytic activity of the BDD electrode is not high as that of sp^2-bonded carbon [21]. Moreover, the production of diamond powder is carried out mainly by the high-pressure high temperature process (HTHP), resulting in challenges to get a properly doped diamond due to crystallographic defects caused by a high content of boron [12]. Indeed, the contamination of the dopant in the synthesized conductive diamond can influence the electrochemical analysis. For these reasons, the hybridized material has been developed, which integrates both sp^2 and sp^3 phases. This material offers a trade-off exists between a wide potential window and relatively high electrocatalytic activity, thus leading to high efficiency and high performance in the detection of analytes.

Recently, a new hybridized material that well integrates both sp^2 and sp^3 phases, boron-doped diamond/graphene nanowalls (DGNW), has been developed by our group [22–24]. The GNWs can be like diamond films *in-situ* doped by boron atoms in the microwave plasma assisted chemical vapor deposition (MWPACVD) process. This process is a catalyst-free-based process, thus making DGNW growth possible on different substrates with no metallic contamination. In addition, the DGNW is a perpendicular carbon wall overgrown by nanodiamond clusters, making them a very promising electrochemical material in terms of high electrocatalytic activity ($k° = 1.1 \times 10^{-2}$ cm s^{-1}) and wide working potential window (up to 3.2 V vs. Ag/AgCl) [23]. Hence, it is worth noting that this material can be employed as an electrode, as it exhibits excellent electrochemical performance for biosensing applications. To the best of our knowledge, the DGNW has not been used as an electrode material to examine neurotransmitters.

Herein, we report an electrochemical sensor based on DGNW for neurotransmitters detection. To be highlighted, this present work mostly focuses on the neurotransmitters in the catecholamine family, i.e., serotonin (5-hydroxytryptamine, 5-HT), epinephrine (adrenaline, EPI), and dopamine (3,4-dihydroxyphenylthylamine, DA), which play an important role in the biological processes of our body [25]. These molecules are responsible for various functions essential to the brain, e.g., behavior and recognition, hormone functions, and establishing human brain-body function [26]. The average levels of 5-HT, EPI, and DA in urine samples are in the range between 0.03 - 0.13 μM, 0 – 0.1 μM, and 0.3–3 μM, respectively [27]. Suppressed levels or the complete depletion of these neurotransmitters can be associated with severe health problems, including Parkinson's and Alzheimer's diseases, schizophrenia, Huntington's disease, or hypertension neuropsychiatric disorders [28]. Accordingly, it is necessary to develop sensitive and selective methods for the determination of neurotransmitters.

A wide range of detection methods has been reported to analyse neurotransmitters, such as colorimetry, mass spectroscopy, chemiluminescence, chromatography, and capillary electrophoresis [29]. However, these techniques require sophisticated training, benchtop operation, and costly and bulky instruments, making these techniques limited the real time analysis and on-site monitoring [30]. To approach the onsite analysis, the miniaturized analytical device has been proposed with electrochemical technique. Screen-printed electrodes (SPEs) have been mostly reported in numerous electrochemical applications because their enable simplicity, portability, inexpensiveness, ease of fabrication, and operation [4,31]. Taking advantage of

these aspects, the SPEs offer mass production and can be implemented with an electrochemical technique for neurotransmitters detection.

In this present study, we propose for the first time using DGNW coupled with screen-printed graphene electrode (SPGE) for electrochemical detection of 5-HT. The DGNWs were prepared using conductive diamond-based powder synthesized from commercially available nonconductive nanodiamond powder. Synthesized DGNW powder shows features between BDD (sp^3 diamond phase) and graphene nanowall (sp^2-bonded carbon phase) on the same surface. Depending on the synthesis conditions, we obtained carbonaceous powder with a different surface resembling morel-like structures in shape. The variety of DGNW shapes can affect their surfaces, chemical composition, and electrochemical properties. The DGNW was coupled with the SPGE using a drop-casting procedure. The surface morphologies of each DGNW type, including scanning electron microscope (SEM) and Raman spectroscopy, are discussed. The electrochemical characteristics of DGNW modified electrode are studied using cyclic voltammetry (CV), and electrochemical impedance spectroscopy (EIS), and compared to the bare SPGE electrode. To quantify the concentration of neurotransmitters, differential pulse voltammetry (DPV) was used. Compared to bare SPGE, the DGNW modified electrodes shows significantly better sensitivity with a low detection limit and reduced fouling effects. Besides, to evaluate the efficiency and applicability of the proposed sensor in real sample analysis, a synthetic urine sample was then tested. This proposed sensor presents simplicity, portability, and high-antifouling capability, and can be applied in a wide range of biological assays.

2. Experimental

The details of the chemical, reagents, apparatus, and measurements, and the preparation of glassy carbon electrode (GCE) and gold disk electrode (GDE) are presented in the supporting information section 1–3.

2.1. Synthesis of boron/nitrogen co-doped diamond-graphene nanowall-structured particles (DGNW)

DGNWs were synthesized using a microwave Plasma Assisted Chemical Vapor Deposition system (MWACVD, SEKI Technotron AX5400S, Japan). In brief, two sets of samples were prepared with and without additional nitrogen in the gas phase. As the substrate, a diamond powder was used with *ca.* 1 μm size (YDY) in an amount of 1 g. The following process conditions: gas mixture—H$_2$, CH$_4$, B$_2$H$_6$, with a total flow of 325 sccm; process pressure—50 Torr; microwave power—1.3 kW; microwave radiation—2.45 GHz. All samples were doped by using diborane (B$_2$H$_6$:1000 H$_2$) as an acceptor precursor. The [B]/[C] ratios in the gas phase were set to 2000 and 5000 ppm, which resulting in the various contents of boron incorporated into nanowalls. During the process, the substrate holder was heated up to 700°C by an induction heater, which was controlled by a thermocouple. Four different DGNW samples were tested in this study. All parameters for DGNW preparation are shown in Table 1. More details about the growth mechanism of DGNW are described in the previous work [23].

Table 1
The condition parameter of the DGNW preparation in this present work.

Sample	[B]/[C] ratio	Additional N$_2$	Growth time
DGNW-2 k N$_2$	2000	Yes	3 h
DGNW-2 k	2000	No	3 h
DGNW-5 k N$_2$	5000	Yes	3 h
DGNW-5 k	5000	No	3 h

2.2. Screen-printed graphene electrode (SPGE) material and fabrications

The screen-printed graphene electrode (SPGE) pattern was fabricated according to a previously described procedure [32]. In short, a three-electrode system was constructed using an in-house screening method on a transparency film as an electrode substrate. The SPGE pattern was designed by AutoCAD software and cut using a laser cutter (GCC C180II) in a transparency film. For electrode fabrication, a graphene-based ink (as the WE, 4 mm in diameter) and counter electrode (as the CE), and Ag/AgCl ink (as the RE) were printed on transparency film. After that, the printed electrode was cured in an oven at 60°C for 1 h to eliminate residual organic solvents in the ink composition. Finally, the SPGE was connected with an alligator clip to perform the electrochemical measurement. The electrode design and schematic illustration of the SPGE electrode are shown in Fig. 1.

2.3. Drop casting for electrode modification

Prior to electrode modification, the 1 mg mL^{-1} of the DGNW powder dispersion in ultrapure water was bath sonicated for 30 min before use. Four different types of DGNW powder were compared, designated DGNW-2k N$_2$, DGNW-2k, DGNW-5k N$_2$, and DGNW-5k. All DGNW types were characterized by SEM and Raman spectroscopy, as shown in Fig. 2A and 2B. To prepare the modified electrode, 8 μL of DGNW suspension in water was dropped on the electrode surface (all electrodes: SPGE, GCE, and GDE) and then kept dry to evaporate the solvent at room temperature for 30 min (the optimization of the amount of DGNW loading and number of drop-casting layers can be found in the supporting information, section 8, and Fig. S5). Finally, the modified electrodes are ready to measure the neurotransmitter.

2.4. Electrochemical of neurotransmitter determination

For the detection of neurotransmitters on SPGE, 100 μL of different concentrations of 5-HT and other neurotransmitters solution were applied to the three-electrode system. A differential pulse voltammogram signal was then monitored in the potential range from -0.3 V to 0.6 V (vs. Ag/AgCl), with a modulation amplitude of 200 mV, a standby potential of 0 V, a step potential of 5 mV, and an equilibration period of 3 s at room temperature.

2.5. Preparation of synthetic urine sample

The preparation of synthetic urine samples was prepared following the previous report [33,34]. Briefly, all reagents which are including CaCl$_2$·2H$_2$O (0.28 g), NaCl (0.73 g), Na$_2$SO$_4$ (0.56 g), KH$_2$PO$_4$ (0.35 g), KCl (0.40 g), NH$_4$Cl (0.24 g), and urea (6.25 g) were prepared in 250 mL of ultrapure water (pH 7.6). It should be noted that the synthetic urine sample was immediately used after its preparation to eliminate other interferences in case of the hydrolysis of urea.

3. Results and discussion

3.1. Surface morphology and structure of DGNW

To characterize the different types of the DGNW several techniques, including high-resolution scanning electron microscope (HR-SEM) and Raman spectroscopy, were carried out. Initially, the surface morphologies of each different DGNW type were characterized using HR-SEM. According to the previously reported, the morphological characteristic of a DGNW is formed in a maze-like shape, with grain-sized in a micrometric range [23]. The production of DGNW affects to the sp^3 (diamond phase) and sp^2 (non-diamond phase) on the material surface, and influences the electrochemical properties, such as surface area, surface morphology, electrocatalytic properties, as well as the double-layer capacitance of DGNW in the electrochemical analysis [35,36]. Here, the diamond powder was modified in the MWPACVD process with and without N$_2$ in the gas composition to obtain the DGNW. SEM images of each DGNW type are presented in Fig. 2A. These changes have a crucial influence on the DGNW growing onto the diamond powder. As shown in Fig. 2A panels I and III, the diamond powder is visibly overgrown by DGNW, creating maze-like or morel-like structures. Likewise, the N$_2$ influences the growth of DGNW in the gas phase and determines the structure 'density' of the GNWs. As expected, the increasing boron content had significantly affected to the quantity and amount of GNWs growth on the substrate. Besides, the obtained DGNWs are shortened, which is in agreement with our previous research [23]. It should be pointed out that the shortened walls of DGNW provide a positive effect, indicating that this material has a high surface area. Contrarily, when there is no additional N$_2$ the DGWN grows poorly; only other forms of sp^2 carbon overgrown the diamond powder (Fig. 2A, panels II and IV). Therefore, we conclude that the difference in [B]/[C] ratios and the presence of N$_2$ in the dop-
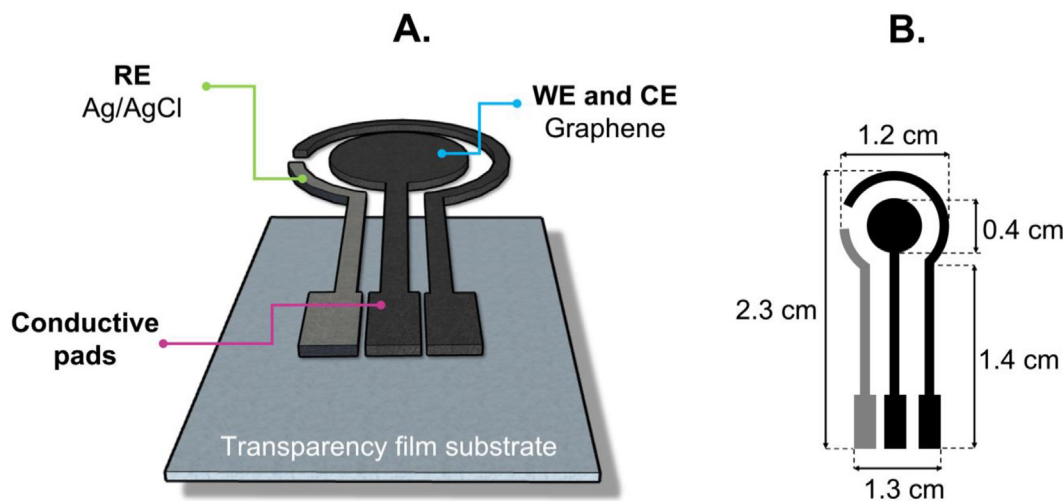

Fig. 1. (A) and (B) schematic illustration of screen-printing graphene electrode (SPGE) for 5-HT detection. The flexible transparency film was used as a substrate. The graphene-based ink and Ag/AgCl ink were screened to create a working electrode (WE, 4 mm in diameter) and counter electrode (CE), and reference electrode (RE), respectively.
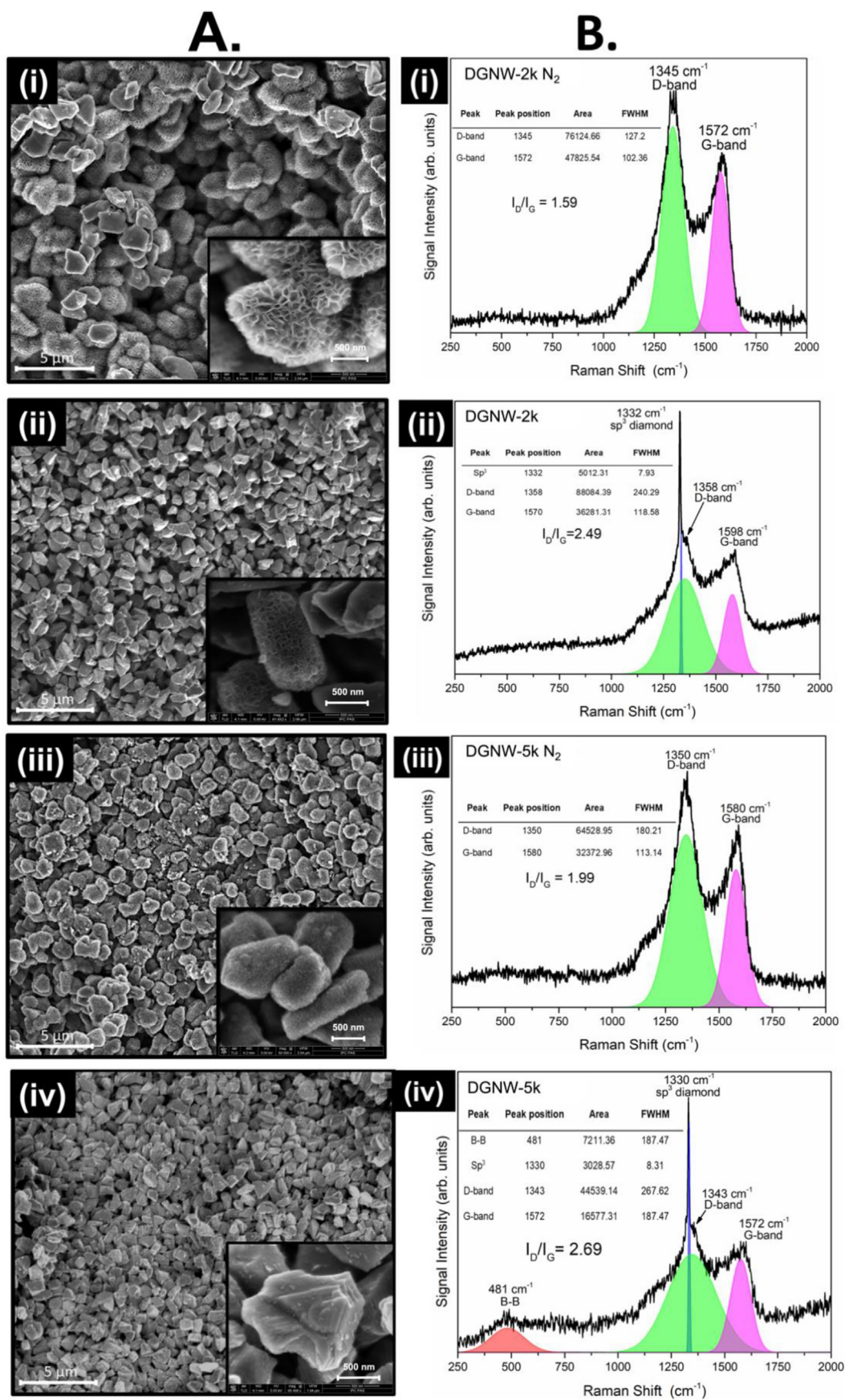
Fig. 2. (A). HR-SEM images and (B). Raman spectra of DGNW with 2000 and 5000 ppm of [B]/[C] and with and without additional nitrogen in the gas phase. The spectral decomposition was achieved by fitting the Gaussian distribution. DGNW-2k N_2 (with N_2, [B]/[C] 2000 ppm), DGNW-2k (without N_2, [B]/[C] 2000 ppm), DGNW-5k N_2 (with N_2, [B]/[C] 5000 ppm), and DGNW-5k (without N_2, [B]/[C] 5000 ppm) are shown in panel (I), (II), (III), and (IV), respectively.

4

ing process of GNWs play the main role in terms of the density and length of DGNW and influence on the quality of the electrode surface, and accordingly to the electrochemical performance.

To confirm the different forms of carbon layers of DGNW, Raman spectroscopy was then carried out (Fig. 2B). The samples with N_2 (DGNW-2k N_2 in panel I and DGNW-5k N_2 in panel III) reveal only two prominent peaks, the D-band located at 1345–1350 cm^{-1} and G-band 1572 – 1580 cm^{-1}, corresponding to the finite crystalline size in A_{1g} mode and E_{2g} mode of sp^2-bonded carbon, respectively. In the second case (DGNW-2k in panel III and DGNW-5k in panel IV), the Raman spectra appear to be a mixture of sp^2 and sp^3 carbon phases (at 1330 – 1332 cm^{-1}), resembling more sp^2 than sp^3 diamond phase. The presence of broad peak of DGNW-5k located at 481 cm^{-1} was associated with the boron-modified carbon nanosheet as shown in Fig. 2B, panel IV. The decomposition by Gaussian distribution also shows differences between samples with and without nitrogen such as larger area under the peaks but smaller full width at half-maximums (FHWM) which also confirms the influence of N_2 on the growth of DGNW. Experimentally, the I_D/I_G of each DGNW type was found to be 1.59 for DGNW-2k N_2, 2.49 for DGNW-2k, 1.99 for DGNW-5k N_2, and 2.69 for DGNW-5k, respectively. The ratios I_D/I_G are significantly smaller for samples with additional N_2 in the growth process compared to no additional N_2. It should be noted that the presence of N_2 during the preparation of DGNW led to a high sp^2 phase and consequently improved the electrical conductivity of the electrode surface. These results are in accordance with the previous work [22,37]. We hypothesize that the difference in surface morphologies of each DGNW clearly evident in SEM and Raman images contributes to the electrochemical behavior as presented in Fig. 3. More details of surface characteriza-tion of this material using X-ray photoelectron spectroscopy (XPS) and molecular composition can be found in previous reports [23,38].

3.2. Electrochemical properties of the DGNW modified electrode

The electrochemical behavior after the modification of each DGNW type onto the electrode surface can be characterized by CV and EIS techniques. According to the literature review, the presence of sp^3 on the BDD electrode exhibits a wide potential window, low back-ground current, high corrosion resistance, and high-antifouling capa-bility [39]. In contrast, a high sp^2 content on the electrode surface could favor the oxidative reaction or the electrocatalytic property of biomolecule compounds [35]. Furthermore, the oxygen reduction reaction (ORR) can occur in the presence of high sp^2 content on the electrode surface, causing an enhancement of the background current and the limit the electrochemical potential window [13,40]. Thus, the integration of sp^3 and sp^2 phases in our system were then verified. CV experiments of the modified SPGE electrode with DGNW were recorded and compared with the bare SPGE electrode by sweeping the potential range between -2.0 and 2.0 V (vs. Ag/AgCl) at 100 mV s^{-1} as presented in Fig. 3a. A lower background current response can be obtained after the DGNW-modified on the SPGE elec-trode surface than that of the bare SPGE electrode, which is correlated with sp^3 content on the DGNW surface. As expected, these results can be confirmed that the DGNW-5 k gives both sp^2 and sp^3 content levels, which can increase the electrocatalytic properties, give a wide poten-tial window, low background current as well as high anti-fouling prop-erties. The received results are in agreement with results revealed by SEM and Raman techniques.
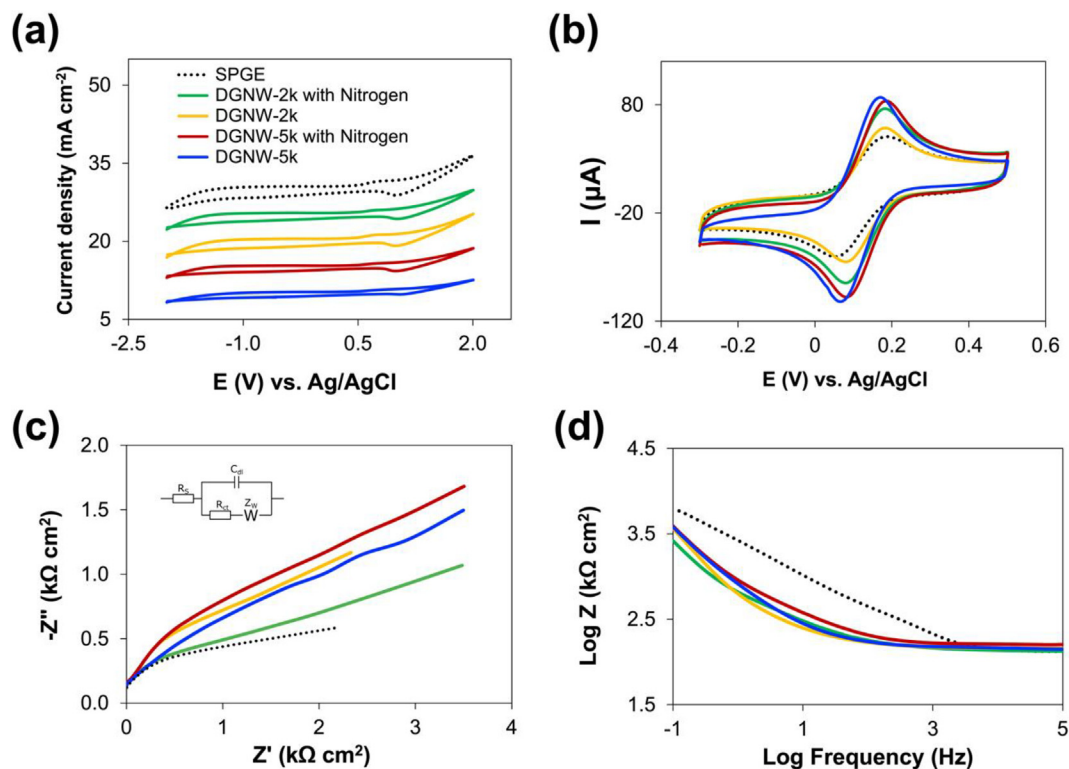

Fig. 3. (a) CVs in the presence of 0.1 M KNO_3, recorded at 0.1 V s^{-1} over the range potential between -2.0 to 2.0 V vs. Ag/AgCl. (b) CVs in the presence of 5 mM Fe$[CN_6]^{3-/4-}$ in 0.1 M KNO_3, recorded over the range potential from -0.3 V to 0.5 V vs. Ag/AgCl. (c) The Nyquist plot and (d) the Bode plot using 5 mM Fe$[CN_6]^{3-/4-}$ in 0.1 M KNO_3, investigated over the frequency range between 0.01 to 10^5 Hz, potential at 0 V vs. Ag/AgCl, amplitude 0.01 V with 6 points per frequency decade, for bare SPGE (dot line), DGNW-2k N_2 (green line), DGNW-2k (yellow line), DGNW-5k N_2 (red line), and DGNW-5k (blue line), respectively. Inset picture: the Randles circuit applied to model EIS data. R_s: electrolyte solution resistance; C_{dl}: constant phase angle element; R_{ct}: interfacial electron transfer resistance; Z_w: Warburg impedance introduced by the diffusion of ions. (For interpretation of the references to colour in this figure legend, the reader is referred to the web version of this article.)

To investigate which DGNW type provides better electrochemical properties, CV was used to measure peak-to-peak separation (ΔE_p) and the electrochemical current repones in the presence of Fe$[CN_6]^{3-/4-}$ as an inner-sphere redox species [41]. This species is an electrochemically reversible redox species. Its redox reaction has been shown to be sensitive to the presence of some surface oxides; therefore, the current response was dependent upon the oxide coverage and cleanliness of the electrode surface. Here, CVs of the modified electrode were compared with the bare SPGE electrode and scanned from -0.3 to 0.5 V (vs. Ag/AgCl) at 100 mV s^{-1} in the presence of 5 mM Fe$[CN_6]^{3-/4-}$ in 0.1 M KNO$_3$. As shown in Fig. 3b, symmetrical voltammograms were obtained, and the calculated ΔE_p values after each DGNW-modified electrode were 109.5 ± 5.6 mV for DGNW-2k N$_2$, 113.5 ± 5.7 mV for DGNW-2k, 109 ± 2.8 mV for DGNW-5k N$_2$, and 104.5 ± 1.4 mV for DGNW-5k, respectively (n = 3). In contrast, the measured ΔE_p value of bare SPGE was 145 ± 10 mV. As expected, after modification with each DGNW type, smaller ΔE_p values of the modified electrode were achieved compared to the SPGE electrode, meaning that the modified electrode exhibited a faster electron transfer rate and greater electrochemical reversibility than that of the bare electrode. These results can also indicate a high level of surface cleanliness and low oxide content on the electrode surface. The measured ΔE_p values are much higher than the theoretical value (59 mV) because of the resistivity of the DGNW layer grown by the CVD process [42]. Nonetheless, the obtained ΔE_p values of the DGNW modified electrode toward Fe$[CN_6]^{3-/4-}$ redox solution are close to those of undoped DGNW electrode materials characterized electrochemically without any electrochemical pretreatment. Likewise, these obtained ΔE_p values are much lower than other pristine CNWs [43–45] or stencil-printed carbon electrode [46]. Note that all of these obtained values are in line with previous work [23].

Moreover, EIS was used to examine insight into electrode kinetics or the change of an electrical property on the electrode surface after DGNW modified electrode by measuring the charge transfer resistance (R_{ct}) between the redox species employed and the electrode surface. This technique provides the data in terms of the Nyquist plot, which including a semicircle part at high frequencies and a straight-line part at low frequencies. The semicircle and the straight-line parts demonstrate the electron transfer efficiency from the electrochemical cell and the behavior of the redox solution from the diffusion-controlled region, respectively. The Nyquist plot of each DGNW modified electrode type is shown in Fig. 3c. After modified each DGNW on the SPGE electrode surface (green line, yellow line, red line, and blue line), a negligibly discernible charge transfer with a long straight line at high frequency was obtained, indicating a high conductivity and superior electron transfer of the DGNW material. The results after modified each DGNW type provide the same trend. In contrast, the narrow straight-line was obtained for the bare SPGE (dot line) at high frequencies. This result indicated that the bare SPGE electrode provides the lowest electron transfer rate and conductivity but increases after modification with DGNW. For better visualization, the bode plot was evaluated in Fig. 3d. Similarly, parallel results were achieved with the Nyquist plot. More information of EIS measurement and the calculation of heterogeneous electron-transfer constant are shown in the supporting information in section 4 – 5, and Fig. S1.

The electroactive surface areas (A_e, cm^2) of the bare electrode and the modified electrode were measured via CV at various scan rates in the presence of 5 mM Fe(CN)$_6^{3-/4-}$ in 0.1 M KNO$_3$ using the Randles-Sevcik equation [11]:

$$i_p = (2.69 \times 10^5) A D^{1/2} n^{3/2} \nu^{1/2} C$$

where i$_p$ is the current response of the bare SPGE electrode or the DGNW modified electrode (amps), D is the diffusion coefficient of Fe(CN)$_6^{3-/4-}$ (cm^2 s^{-1}), ν is the scan rate (V s^{-1}), and C is the concentration of Fe(CN)$_6^{3-/4-}$ (M). The calculated A_e values were found to be 0.0126 cm^2 for bare SPGE electrode, 0.0167 cm^2 for DGNW-2k N$_2$, 0.0155 cm^2 for DGNW-2k, 0.0178 cm^2 for DGNW-5k N$_2$, and 0.0184 cm^2 for DGNW-5k modified electrodes, respectively. These increases in the A_e values could imply the successful modification of DGNW on the bare SPGE electrode surface through the physical chemistry (drop-casting procedure). Besides, the increase in the electrochemical current response was caused by a high surface area of DGNW as the component of the electrochemical system. More details can be found in the supporting information (section 6, Fig. S2).

3.3. Electrochemical current response of 5-HT on the modified electrode

As proof of concept, the electrochemical behavior of 5-HT on the bare SPGE electrode and the DGNW modified electrode using DGNW-5k were evaluated by CV and DPV techniques. As shown in Fig. 4a and 4b, the voltammogram results clearly show that this 5-HT studied typically gave an ill-defined oxidation peak at 0.37 V vs. Ag/AgCl with a large background current at the unmodified SPGE electrode (black line). Meanwhile, the DGNW modified electrode (blue line) provides a well-defined peak at 0.25 V vs. Ag/AgCl and current significantly higher compared to that of the bare SPGE. These results suggested that the DGNW modified electrode could combine with SPGE to improve the sensitivity and the detection limit for the determination of neurotransmitters.

To confirm a diffusion-controlled process, the electrochemical processes of 5-HT on the DGNW modified and unmodified electrodes were further examined by CV at various scan rates (25 – 100 mV s^{-1}) as presented in Fig. 4c–d. The logarithm of oxidative current response of 5-HT of the modified electrode increases linearity with the logarithm of scan rate, indicating that the electrochemical process is a diffusional control. As displayed in Fig. 4e, the slopes were found to be 0.54 for bare SPGE and 0.55 for DGNW-5k modified electrode, respectively. More details can be found in the supporting information in section 7, Fig. S3. It should be noted that the theoretical slope value was equal to 0.5 for a purely diffusion process [22]. These obtained values were close to the theoretically expected value of a diffusion-controlled process. Thus, the electro-oxidation of 5-HT was controlled by a diffusion process.

Next, electrochemical current responses of the bare electrode and each DGNW modified electrode type were evaluated to confirm the proposed method. The oxidative current responses of 5-HT using the DPV technique were investigated with a scanned potential range of -0.3 V to 0.6 V (vs. Ag/AgCl) at the DGNW-modified SPGE electrodes and compared with the bare SPGE electrode. As shown in Fig. 4f, an increase in the current response in the presence of 5-HT could be observed at the DGNW-modified electrode. In comparison with the bare SPGE electrode, the oxidative current responses of DGNW-2k N$_2$, DGNW-5k N$_2$, and DGNW-5k modified electrode were obtained to be significantly higher (2–3 times) than that of the non-modified electrode. Meanwhile, the DGNW-2k modified on the SPGE electrode provides a similar current response to the bare SPGE electrode. The higher current response in the presence of DGNW could possibly be attributed to the high surface area and efficient electron transport of the DGNW material, which potentially improved the degree of 5-HT oxidation reaction [16,47]. We further considered the oxidative current responses in the presence of 5-HT of each DGNW modified electrode on GCE and GDE, bare GCE, and bare GDE electrode. More details are shown in the supporting information (Fig. S4). Briefly, the current response of the DGNW modified on the SPGE electrode provides a higher current response for 5-HT detection over the DGNW modified on GCE and GDE electrodes, indicating a high sensitivity of the electrode platform. Considering all the results mentioned above, it certainly indicates that the DGNW-5k modified on the SPGE electrode demonstrates the highest sensitivity for 5-HT detection. Hence, a DGNW-5k and SPGE electrode were selected for subsequent experiments.
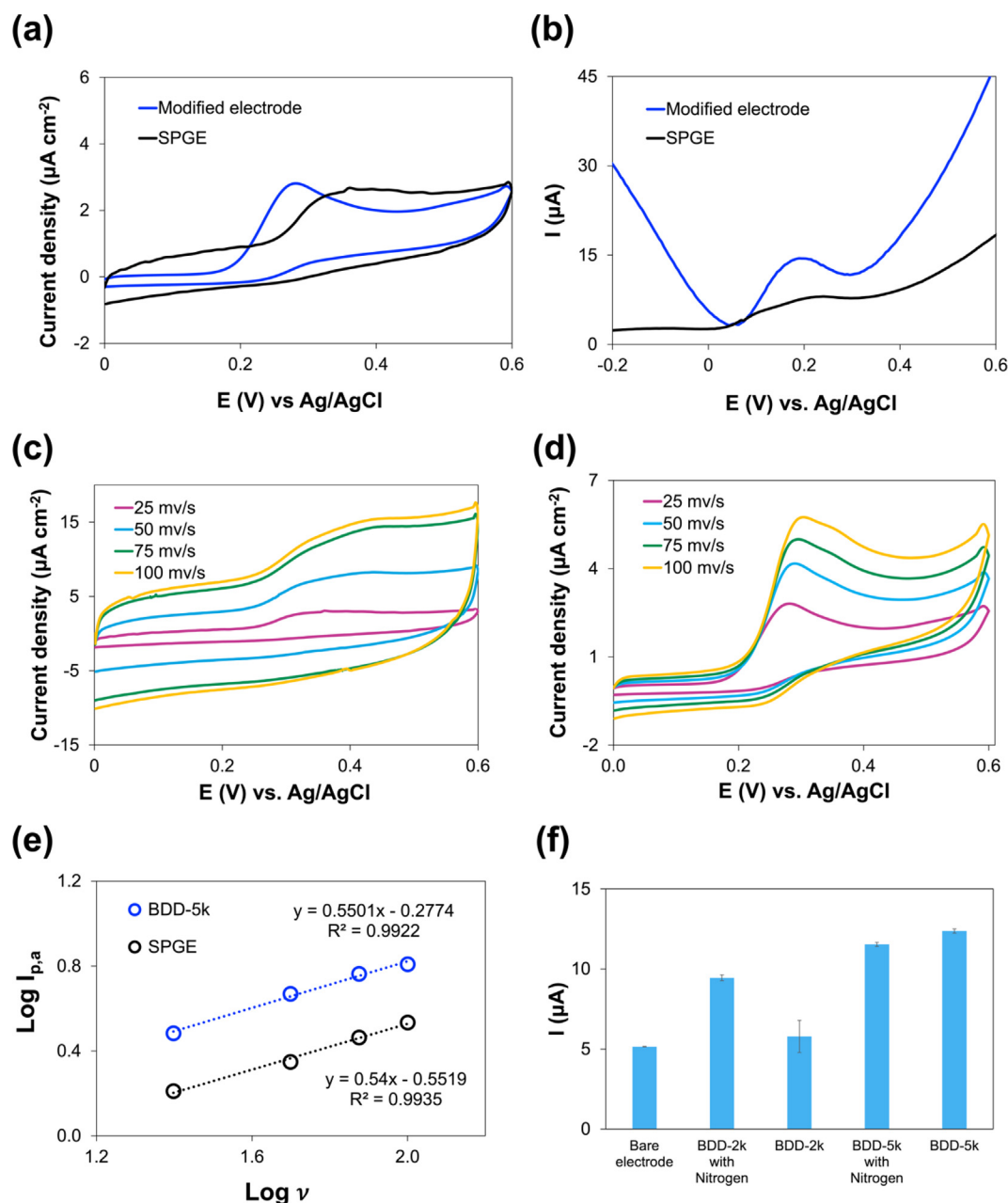
Fig. 4. (a) CVs and (b) differential pulse voltammograms in the presence of 50 μM 5-HT for bare SPGE (black line) and DGNW modified on the SPGE (DGNW-5k, blue line). (c) CVs of bare SPGE and (d) DGNW modified electrode recorded as a function of a series of scan rate using 50 μM 5-HT , (e) The relationship between the logarithm of oxidative current response (log $I_{p,a}$) and logarithm of scan rate (log ν), and (f) The comparison of the oxidative current response before and after modified various DGNW types on SPGE using 100 μM of 5-HT. The error bar represents the standard deviation calculated from three replicated measurements (n = 3). (For interpretation of the references to colour in this figure legend, the reader is referred to the web version of this article.)

3.4. Optimization

In this work, various parameters, such as the amount of DGNW loading and the number of drop-casting layer, affecting the sensitivity and the electrochemical performance of the proposed sensor were investigated to obtain the high sensing efficacy for 5-HT detection. The optimization parts were carried out with DGNW-5 k modified electrode. Briefly, the optimal conditions were as follow: 1 mg mL^{-1} of the amount of DGNW loading and 2 drop-casting layers. The discussion and more details can be found in the supporting information (section 8, Fig. S5).

3.5. Analytical performance

The analytical performance of the electrochemical sensor for the 5-HT sensor was evaluated using both the DGNW-5k modified and bare SPGE. As illustrated in Fig. 5, the electrochemical current response of the DGNW modified on the SPGE electrode (red line, Fig. 5a) proportionally increases with increasing concentration of 5-HT in the range of 1 – 500 μM (I = 0.1245 $C_{5\text{-HT}}$ (μM) + 1.2724, R^2 = 0.993) with a limit of detection (LOD = 3SD/slope) of 0.28 μM. For the bare SPGE electrode (green line, Fig. 5a), the calibration plot shows a linear response in the range of 5 – 500 μM (I = 0.0644 $C_{5\text{-HT}}$ (μM) −
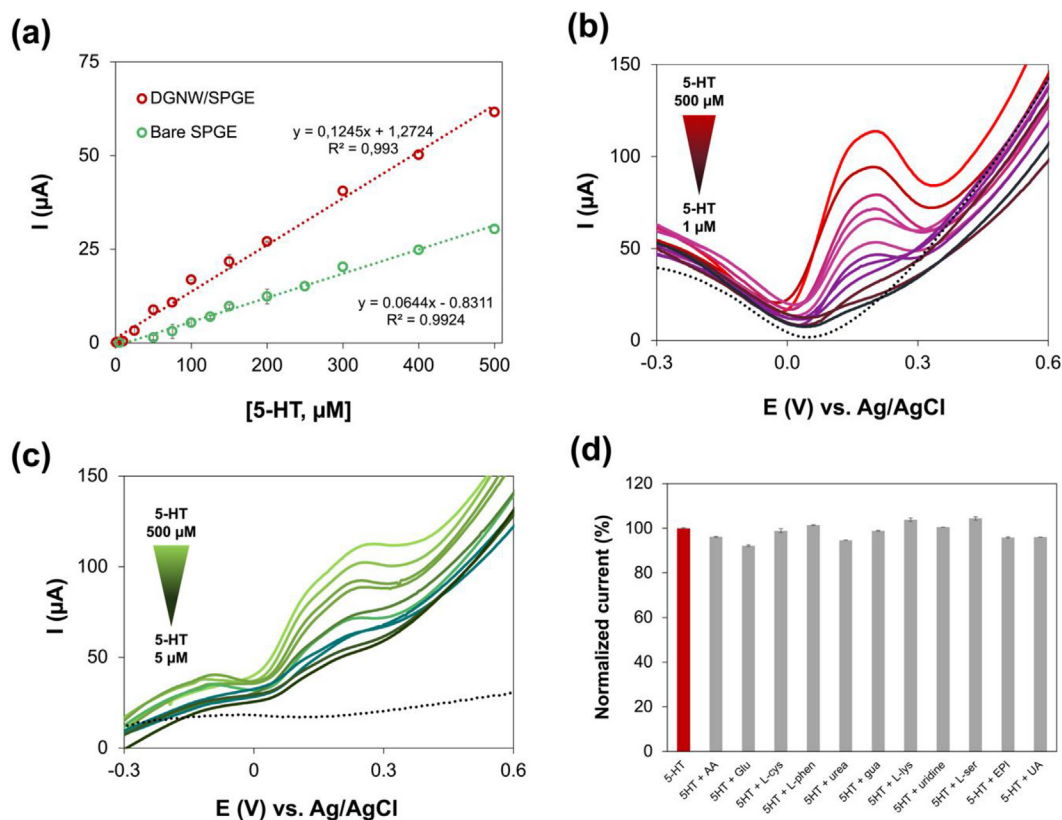
Fig. 5. (a) linear relationship between the oxidative current response and the concentration of 5-HT of bare SPGE (green line) and DGNW modified electrode (red line). (b) differential pulse voltammograms of the DGNW modified electrode and (c) bare SPGE tested at different concentrations of 5-HT ranging from 1 μM to 500 μM and 5 μM to 500 μM, respectively. (d) the influence of other interferences on the current response of 5-HT and the current response was calculated in terms of normalized current to correct the background of each interference. The error bar represents the standard deviation calculated from three replicated measurements (n = 3). (For interpretation of the references to colour in this figure legend, the reader is referred to the web version of this article.)

0.8311, R^2 = 0.9924) with a limit of detection (LOD = 3SD/slope) of 1.23 μM. The oxidative current response plotted at different concentrations of 5-HT using a modified electrode and the bare SPGE are presented in Fig. 5b and Fig. 5c, respectively. We also evaluated and compared the analytical performance on GDE and GCE for 5-HT detection; all results are shown in the supporting information (section 9, Fig. S6). Moreover, a comparison of the analytical performance between previously reported methods and the proposed sensor modified with DGNW for 5-HT detection is shown in Table 2. Among the methods, our approached sensor provided a high-antifouling electrode, acceptable LOD, wide dynamic range, disposability, and ease to operation with the lowest cost for 5-HT determination. Although, other reports show superior performance with lower LODs, most of them require complicated and notable materials for modification steps, and expensive electrode materials. Additionally, the performance of the proposed sensor is sufficient to detect 5-HT in urine and serum sample (normal range between 0.27 and 1.65 μM), thereby making our proposed format for an alternative point-of-care application.

To verify the reproducibility, five DGNW modified SPGE electrodes under the same conditions were used to detect 5-HT at different concentrations. The relative standard deviations (RSDs) of the electrochemical current response are less than 10 % (in the rage of 5.36 to 9.43 %), indicating satisfactory reproducibility of the developed electrode.

We further investigated the influence of other proteins and biomolecules that can be found in urine samples. Other interferences, such as epinephrine (EPI), uridine, urea, uric arid (UA), ascorbic acid (AA), guanine (Gua), L-cysteine (L-Cys), L-serine (L-ser), L-lysine (L-Lys),

L-phenylalanine (L-Phen), and glutamine (Glu), were employed in this study. All interferences were prepared in PBS buffer and diluted in a proper concentration. The results can be seen in Fig. 5d. As expected, the change in DPV current response was only obtained when 5-HT is present in the system. Contrarily, no significant changes (generating merely less than ± 10 % of the error) were obtained from other interferences even in 10-fold excess of EPI and UA, 40-fold of AA, and 100-fold of other interferences greater concentrations (More details are provided in the supporting information in section 10, Table S2 and Fig. S7). Consequently, it can be concluded that the proposed electrode provides a good selectivity and specificity toward targeted 5-HT.

We additionally evaluated the storage stability. The modified electrode and the SPGE were prepared and stored in a closed container at room temperature (22 ± 2 °C). As shown in Fig. S8a, the results show that the modified electrode can preserve its activity for at least 1 month while causing a signal change less than 10 % (the normalized currents are retained in the range from 92.95 % to 103.76 %) with %RSDs less than 10 % (3.73 % to 6.72 %). On the other hand, there was no distinct change in the normalized current after storage of the SPGE in dry conditions for over 8 weeks (ca. 2 months) (the normalized currents are obtained in the range from 95.41 % to 105.71 % with %RSDs ranging from 5.28 % to 9.68 %), as presented in Fig. S8b. Therefore, a DGNW modified electrode and SPGE can maintain the constant response as the initiation for more than 1 month and 2 months, respectively.

3.6. anti-fouling properties

Electrode fouling is a major problem of the electrochemical detection of neurotransmitters, such as 5-HT, DA, and EPI. The oxidation

Table 2

A comparison of the analytical performance between the previously reported methods and the proposed sensor using DGNW for 5-HT detection.

Modified electrode materials	Detection technique	Linear range (μM)	LOD (μM)	Number of measurement (scans)	Ref.
G/p-AHNSA/SPCE	SWV	0.05 – 150	0.003	2	[48]
SWCNTs/SPCE	DPV	1 – 2500	0.4	Not specified	[49]
PPyNPs-AuNPs/SPGE	SWV	0.1 – 15	0.0332	Not specified	[50]
PEDOTNTs/rGO/AgNPs/GCE	DPV	0.01 – 500	0.0001	5	[51]
5-HTP/GCE	DPV	5 – 35	1.7	Not specified	[52]
CNT-IL/GCE	DPV	5 – 900	2	Not specified	[53]
AuAg-G/ITO	Amperometry	0.0027 – 4.82	0.0016	Not specified	[54]
MWNTs-ZnO/CS/ITO	SWV	0.1 – 1	0.01	Not specified	[55]
Capt/TP/GE	ASDPV	4 – 250	0.028	Not specified	[56]
	EIS	0.002 – 3.5	0.0012		
pBDD	FSCV	0.05 – 1	0.05	1	[57]
CNTN					
BDDPE	DPV	0.25 – 7.5	0.5	3	[11]
DGNW/SPGE	DPV	1 – 500	0.28	15	This work
SPGE		5 – 500	1.23	2	

Abbreviation: Graphene (G), poly-4-amino-3-hydroxyl-1-naphthalenesulfonic acid (p-AHNSA), Screen-printed graphene electrode (SPCE), Screen-printed graphene electrode (SPGE), Glassy carbon electrode (GCE), Indium tin oxide electrode (ITO), Single-wall carbon nanotube (SWCNTs), Polypyrrole nanoparticle decorated with gold nanoparticles (PpyNPs-AuNPs), Poly (3,4-ethylene dioxythiophene)-reduced graphene oxide-silver Hybridge nanocomposite (PEDOTNTs/rGO/AgNPs), 5-hydroxytryptophan (5-HTP), Carbon Nanotube-Ionic liquid composite (CNT-IL), Graphene encapsulate gold and silver alloy (AuAg-G), Multiwall nanotubes-zinc oxide/chitosan composite (MWNTs-ZnO/CS), Gold electrode (GE), Captopril/thiophenol (Capt/TP), Anodic stripping differential pulse voltammetry (ASDPV), polycrystalline boron-doped diamond (pBDD), Pristine carbon nanotube networks (CTNT), Fast-scan cyclic voltammetry (FSCV), Boron-doped diamond paste electrode (BDDPE).

reaction of these analytes is a surface adsorption dependent two-electron and two-proton process, which can undergo to hydroxylated products for 5-HT [58], leucodopaminechrome for DA [59], leucoepinephrinechrome for EPI [60], and dimers or other electroactive species. In addition, the adsorption onto the electrode surface of these by-products and neurotransmitters itself can create the insulating layer and block or retard the electron transfer through the electrode surface, thus leading to a decrease in the electrochemical current response. To verify the resistance of the DGNW electrode into electrode fouling, the consecutive measurements of DPV in the presence of neurotransmitters were therefore carried out on the modified DGNW and unmodified electrodes (SPGE). The current responses of both electrodes were obtained in the determination 50 μM of 5-HT, EPI, and DA by using the same electrode in each repeated measurement without any pretreatment steps. Fifteen consecutive DPVs in the presence of neurotransmitters were monitored as a function of the normalized current responses with respect to the first DPV over the scan number are shown in Fig. 6. After 15 consecutive scans, the current responses of the unmodified electrode (black line) continuously decreased to 19.06 % of 5-HT and 59.47 % of EPI, and constantly increased to 151.46 % of DA from the initial value, respectively. The obtained results of the unmodified electrode show a greater degree of adsorption of neurotransmitters products and dimers film on the electrode surface than that of the modified electrode. The fluctuation in the current response of the bare SPGE could possibly be explained by the oxidation reaction of neurotransmitter that generates hydroquinone, dimers, and other electroactive species [61]. This product can possibly produce an electrochemical current response and adsorb onto the electrode surface [62]. In the meantime, the current responses of the DGNW modified electrode (blue line, green line, and red line in Fig. 6a–c) provided relatively constant for at least 15 scans compared to the bare SPGE electrode. Consequently, the modified electrode has a maximal anti-fouling capability for analysis of neurotransmitters up to 15 measurements. The comparison of the differential pulse voltammograms between the 1st (solid line) and 15th scans (dash line) of the modified and unmodified electrode are shown in the right-hand side of Fig. 6. Considering all obtained results, compared to the bare SPGE electrode, the presence of DGNW exhibits a wider electrochemical potential window, lower background current response, and is able to circumvent the fouling of neurotransmitters, such as 5-HT, EPI, and DA, respectively.

In addition, a pretreatment method was applied to reactivate the electrode surface and enhance the resistance to electrode fouling. According to previously reported results [11,16], an anodic pretreatment on the DGNW modified electrode was tested and compared the DPV results in the presence of 50 μM 5-HT between before and after pretreatment. The modified electrode was tested for 15 consecutive cycles before the beginning of pretreatment with 0.01 M PBS buffer at 1.5 V (vs. Ag/AgCl). As presented in Fig. S9, the voltammograms after pretreatment at different times in the range of 60 s to 300 s (Fig. S9b–f, orange line, yellow line, green line, red line, and blue line) on the same electrode without any cleaning steps were performed and compared with the first voltammogram of 5-HT detection (black line). As expected (Fig. S9a), the current responses after anodic pretreatment were similar to those of the fresh DGNW modified electrodes at 240 s. These results demonstrated that the DGNW modified electrode was reactivated to its original state after this pretreatment procedure. Therefore, this anodic pretreatment was proposed as an alternative way to refresh the electrode surface for 5-HT and other neurotransmitters in the future.

3.7. Electrochemical detection of serotonin in the synthetic urine sample

Eventually, the proposed sensor was employed to evaluate the applicability of the method for 5-HT detection in the synthetic urine sample by using a standard addition method. A series of synthetic urines with known amounts of spiked 5-HT in the range from 30 to 250 μM were used to create a linear calibration plot. As exhibited in Fig. S10, there is no significant difference in slope (m) between the standard calibration curve (black line) and standard addition curve (blue line), meaning that a negligible effect from other interferences and matrices presented in the urine sample. Moreover, the %recoveries and %RSDs of 5-HT in synthetic urine samples were determined to be in the ranges of 95.55 % to 102.43 % and 0.42 % to 1.14 %, respectively. The obtained results are summarized in table S3. Based on these results mentioned above, it can be concluded that the developed sensor based on DGNW modified electrode has favorable application prospects to be used for quantitative 5-HT in the biological sample without a complicated modification step. Also, this proposed electrochemical sensor can be capable as an alternative electrode material that increases the electrochemical signal as well as an anti-fouling electrode for in vivo monitoring neurotransmitters in the future.
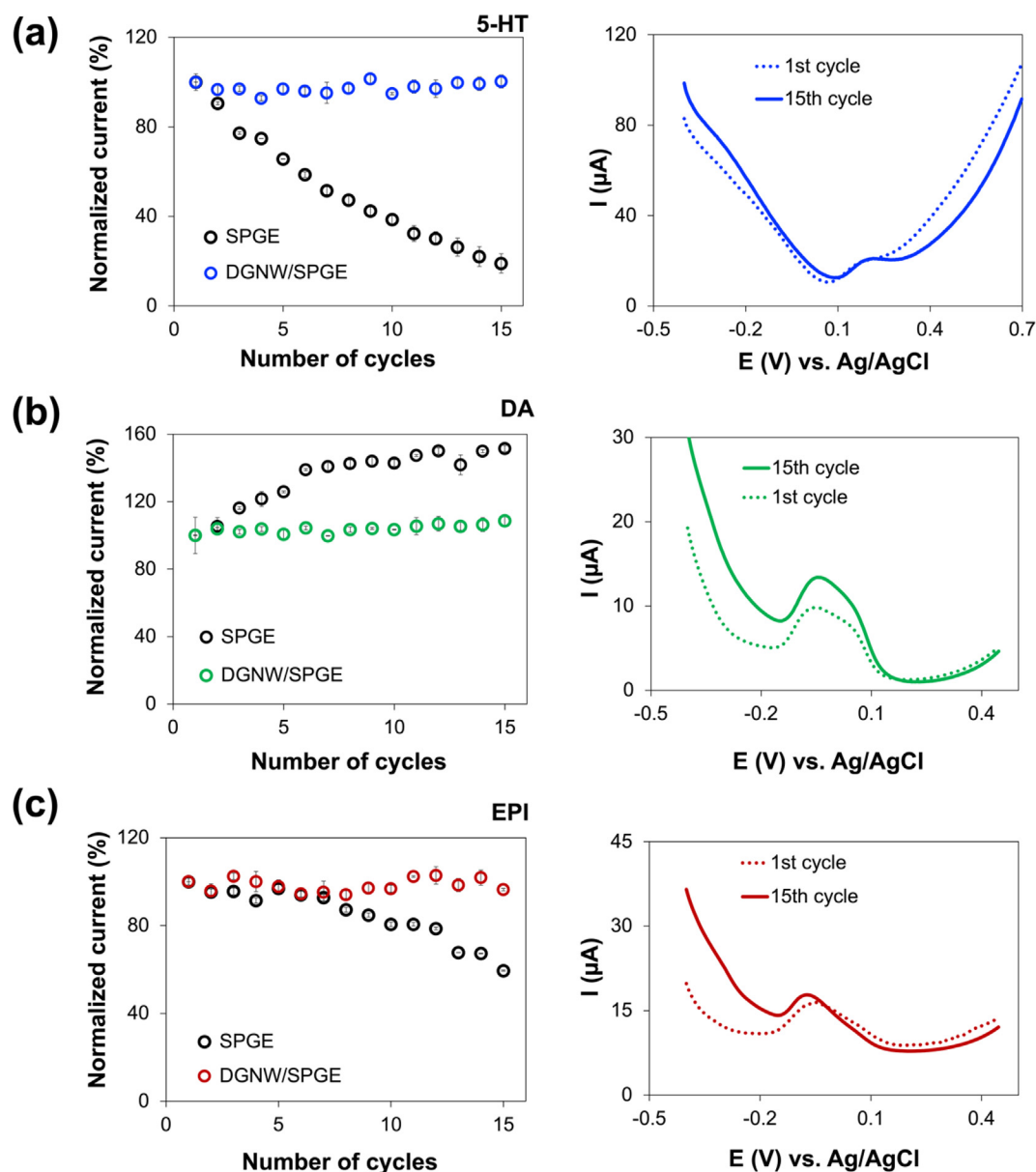
Fig. 6. Left: Plots between differential pulse voltammetric normalized current of 50 μM (a) 5-HT, (b) DA, and (c) EPI and number of consecutive measurements using the DGNW modified electrode (blue line, green line, and red line for 5-HT, DA, and EPI, respectively) and bare SPGE (black line). Right: The comparison of differential pulse voltammograms before (1st scan, dash line) and after successive measurement (solid line) of 5-HT, DA, and EPI. Note that the first peak current response measured in each case has been normalized to 100 %. The signals are shown as means of the measured values (n = 3). (For interpretation of the references to colour in this figure legend, the reader is referred to the web version of this article.)

4. Conclusion

We demonstrated portable electrochemical sensing for the determination of serotonin (5-HT) using DGNW coupled with SPGE for the first time. Herein, two hybridized carbon materials, sp^2 and sp^3 carbon hybridized phases, were explicitly produced to enable an excellent electrochemical property and anti-fouling capability. The DGNW modified electrode was prepared via a drop-casting procedure. This proposed sensor presented a good performance as a cost-effective, sensitive, and selective sensor, which can be used as an alternative detection method of neurotransmitters in the catecholamine family. Under the optimized conditions, DGNW-5k was selected as its enhanced the oxidative current response, improved the sensitivity, and had good antifouling capability. The sensor presented a linear

dynamic range of 1 – 500 μM with a LOD of 5-HT was found to be 0.28 μM. Even though the obtained LOD value was relatively high by this platform, the developed sensor is sensitive enough to analyze 5-HT in a real sample without any pretreatment methods and complicated modifications. Additionally, electrode fouling from the electrooxidation of 5-HT, DA, and EPI is easily overcome through an anodic pretreatment, making this electrode use for multiple measurement (i.e., measuring of 15 samples in situ by using only one electrode). To verify the feasibility, the DGNW modified electrode was applied for 5-HT detection in a synthetic urine sample with standard addition method. The results demonstrated that this platform showed satisfactory %recovery and %RSDs values. Not only the sensitivity and selectivity can be achieved, but this platform also exhibited an excellent anti-fouling capability, as well as high reproducibility, and can

possibly be fabricated in large-scale industry. Consequently, the utility of this sensor can be further extended to other biological molecules and biomarkers of interest.

CRediT authorship contribution statement

Suchanat Boonkaew: Conceptualization, Methodology, Investigation, Validation, Data curation, Formal analysis, Writing – original draft. **Anna Dettlaff:** Investigation, Resources, Writing – original draft, Writing – review & editing. **Michał Sobaszek:** Investigation, Resources, Writing – original draft, Writing – review & editing. **Robert Bogdanowicz:** Project administration, Funding acquisition, Investigation, Resources, Writing – review & editing. **Martin Jönsson-Niedziółka:** Project administration, Conceptualization, Funding acquisition, Writing – review & editing, Supervision.

Data availability

No data was used for the research described in the article.

Declaration of Competing Interest

The authors declare that they have no known competing financial interests or personal relationships that could have appeared to influence the work reported in this paper.

Acknowledgment

Appendix A. Supplementary data

Supplementary data to this article can be found online at https://doi.org/10.1016/j.jelechem.2022.116938.

References

[1] J. Liu, R. Li, B. Yang, Carbon Dots: A New Type of Carbon-Based Nanomaterial with Wide Applications, ACS Cent. Sci. 6 (12) (2020) 2179–2195.

[2] M. Zhou, Z. Zhai, L. Liu, C. Zhang, Z. Yuan, Z. Lu, B. Chen, D. Shi, B. Yang, Q. Wei, N. Huang, X. Jiang, Controllable synthesized diamond/CNWs film as a novel nanocarbon electrode with wide potential window and enhanced S/B ratio for electrochemical sensing, Appl. Surf. Sci. 551 (2021) 149418.

[3] P. Bollella, G. Fusco, C. Tortolini, G. Sanzò, G. Favero, L. Gorton, R. Antiochia, Beyond graphene: Electrochemical sensors and biosensors for biomarkers detection, Biosens. Bioelectron. 89 (2017) 152–166.

[4] A.A. Kava, C. Beardsley, J. Hofstetter, C.S. Henry, Disposable glassy carbon stencil printed electrodes for trace detection of cadmium and lead, Anal. Chim. Acta 1103 (2020) 58–66.

[5] J.J. Gooding, Nanostructuring electrodes with carbon nanotubes: A review on electrochemistry and applications for sensing, Electrochim. Acta 50 (15) (2005) 3049–3060.

[6] J. Yang, J. Yan, R. Chen, H. Ni, Photo-Refreshable Electrochemical Sensor Based on Composite Electrode of Carbon Nanotubes and TiO2 Nanoparticles, IEEE Sens. J. 19 (9) (2019) 3212–3216.

[7] Q.-K.-L. Yao Meng-Ting, M. Zheng-Fang, C. Rong-Sheng, Fabrication of Carbon Quantum Dots Decorated TiO2 Nanotube Arrays for Photoelectrochemical Determination of 5-Hydroxytrptamine, Chin. J. Anal. Chem. 49 (12) (2021) 2005–2014.

[8] B. Wu, S. Yeasmin, Y. Liu, L.-J. Cheng, Sensitive and selective electrochemical sensor for serotonin detection based on ferrocene-gold nanoparticles decorated multiwall carbon nanotubes, Sens. Actuators, B 354 (2022) 131216.

[9] F. Bohlooli, A. Yamatogi, S. Mori, Manganese oxides/carbon nanowall nanocomposite electrode as an efficient non-enzymatic electrochemical sensor for hydrogen peroxide, Sens. Bio-Sens. Res. 31 (2021) 100392.

[10] R.C. Engstrom, Electrochemical pretreatment of glassy carbon electrodes, Anal. Chem. 54 (13) (1982) 2310–2314.

[11] S. Nantaphol, R.B. Channon, T. Kondo, W. Siangproh, O. Chailapakul, C.S. Henry, Boron Doped Diamond Paste Electrodes for Microfluidic Paper-Based Analytical Devices, Anal. Chem. 89 (7) (2017) 4100–4107.

[12] G.F. Wood, C.E. Zvoriste-Walters, M.G. Munday, M.E. Newton, V. Shkirskiy, P.R. Unwin, J.V. Macpherson, High pressure high temperature synthesis of highly boron doped diamond microparticles and porous electrodes for electrochemical applications, Carbon 171 (2021) 845–856.

[13] S.J. Cobb, Z.J. Ayres, J.V. Macpherson, Boron Doped Diamond: A Designer Electrode Material for the Twenty-First Century, Annu. Rev. Anal. Chem. 11 (1) (2018) 463–484.

[14] K. Pungjunun, S. Chaiyo, I. Jantrahong, S. Nantaphol, W. Siangproh, O. Chailapakul, Anodic stripping voltammetric determination of total arsenic using a gold nanoparticle-modified boron-doped diamond electrode on a paper-based device, Microchim. Acta 185 (7) (2018) 324.

[15] E. Majid, K.B. Male, J.H.T. Luong, Boron Doped Diamond Biosensor for Detection of Escherichia coli, J. Agric. Food. Chem. 56 (17) (2008) 7691–7695.

[16] B.V. Sarada, T.N. Rao, D.A. Tryk, A. Fujishima, Electrochemical Oxidation of Histamine and Serotonin at Highly Boron-Doped Diamond Electrodes, Anal. Chem. 72 (7) (2000) 1632–1638.

[17] P. Joshi, P. Riley, K.Y. Goud, R.K. Mishra, R. Narayan, Recent advances of boron-doped diamond electrochemical sensors toward environmental applications, Curr. Opin. Electrochem. 32 (2022) 100920.

[18] S. Nantaphol, O. Chailapakul, W. Siangproh, A novel paper-based device coupled with a silver nanoparticle-modified boron-doped diamond electrode for cholesterol detection, Anal. Chim. Acta 891 (2015) 136–143.

[19] M.C. Granger, M. Witek, J. Xu, J. Wang, M. Hupert, A. Hanks, M.D. Koppang, J.E. Butler, G. Lucazeau, M. Mermoux, J.W. Strojek, G.M. Swain, Standard Electrochemical Behavior of High-Quality, Boron-Doped Polycrystalline Diamond Thin-Film Electrodes, Anal. Chem. 72 (16) (2000) 3793–3804.

[20] B.A. Patel, X. Bian, V. Quaiserová-Mocko, J.J. Galligan, G.M. Swain, In vitro continuous amperometric monitoring of 5-hydroxytryptamine release from enterochromaffin cells of the guinea pig ileum, Analyst 132 (1) (2007) 41–47.

[21] Z. Zhai, N. Huang, B. Yang, C. Wang, L. Liu, J. Qiu, D. Shi, Z. Yuan, Z. Lu, H. Song, M. Zhou, B. Chen, X. Jiang, Insight into the Effect of the Core-Shell Microstructure on the Electrochemical Properties of Undoped 3D-Networked Conductive Diamond/Graphite, J. Phys. Chem. C 123 (14) (2019) 6018–6029.

[22] K. Siuzdak, M. Ficek, M. Sobaszek, J. Ryl, M. Gnyba, P. Niedziałkowski, N. Malinowska, J. Karczewski, R. Bogdanowicz, Boron-Enhanced Growth of Micron-Scale Carbon-Based Nanowalls: A Route toward High Rates of Electrochemical Biosensing, ACS Appl. Mater. Interfaces 9 (15) (2017) 12982–12992.

[23] M. Sobaszek, K. Siuzdak, J. Ryl, M. Sawczak, S. Gupta, S.B. Carrizosa, M. Ficek, B. Dec, K. Darowicki, R. Bogdanowicz, Diamond Phase (sp3-C) Rich Boron-Doped Carbon Nanowalls (sp2-C): Physicochemical and Electrochemical Properties, J. Phys. Chem. C 121 (38) (2017) 20821–20833.

[24] P. Niedziałkowski, Z. Cebula, N. Malinowska, W. Białobrzeska, M. Sobaszek, M. Ficek, R. Bogdanowicz, J.S. Anand, T. Ossowski, Comparison of the paracetamol electrochemical determination using boron-doped diamond electrode and boron-doped carbon nanowalls, Biosens. Bioelectron. 126 (2019) 308–314.

[25] M.D. Tezerjani, A. Benvidi, A. Dehghani Firouzabadi, M. Mazloum-Ardakani, A. Akbari, Epinephrine electrochemical sensor based on a carbon paste electrode modified with hydroquinone derivative and graphene oxide nano-sheets: Simultaneous determination of epinephrine, acetaminophen and dopamine, Measurement 101 (2017) 183–189.

[26] K. Khoshnevisan, E. Honarvarfard, F. Torabi, H. Maleki, H. Baharifar, F. Faridbod, B. Larijani, M.R. Khorramizadeh, Electrochemical detection of serotonin: A new approach, Clin. Chim. Acta 501 (2020) 112–119.

[27] A.J. Steckl, P. Ray, Stress Biomarkers in Biological Fluids and Their Point-of-Use Detection, ACS Sensors 3 (10) (2018) 2025–2044.

[28] B.J. Venton, Q. Cao, Fundamentals of fast-scan cyclic voltammetry for dopamine detection, Analyst 145 (4) (2020) 1158–1168.

[29] Z. Tavakolian-Ardakani, O. Hosu, C. Cristea, M. Mazloum-Ardakani, G. Marrazza, Latest Trends in Electrochemical Sensors for Neurotransmitters: A Review, Sensors (Basel) 19(9) (2019) 2037.

[30] S. Boonkaew, S. Chaiyo, S. Jampasa, S. Rengpipat, W. Siangproh, O. Chailapakul, An origami paper-based electrochemical immunoassay for the C-reactive protein using a screen-printed carbon electrode modified with graphene and gold nanoparticles, Microchim. Acta 186 (3) (2019) 153.

[31] S. Boonkaew, A. Yakoh, N. Chuaypen, P. Tangkijvanich, S. Rengpipat, W. Siangproh, O. Chailapakul, An automated fast-flow/delayed paper-based platform for the simultaneous electrochemical detection of hepatitis B virus and hepatitis C virus core antigen, Biosens. Bioelectron. 193 (2021) 113543.

[32] S. Boonkaew, I. Jang, E. Noviana, W. Siangproh, O. Chailapakul, C.S. Henry, Electrochemical paper-based analytical device for multiplexed, point-of-care detection of cardiovascular disease biomarkers, Sens. Actuators, B 330 (2021) 129336.

[33] L.O. Orzari, R. Cristina de Freitas, I. Aparecida de Araujo Andreotti, A. Gatti, B.C. Janegitz, A novel disposable self-adhesive inked paper device for electrochemical sensing of dopamine and serotonin neurotransmitters and biosensing of glucose, Biosens. Bioelectron. 138 (2019) 111310.

[34] A.M. Campos, P.A. Raymundo-Pereira, C.D. Mendonça, M.L. Calegaro, S.A.S. Machado, O.N. Oliveira, Size Control of Carbon Spherical Shells for Sensitive Detection of Paracetamol in Sweat, Saliva, and Urine, ACS Appl. Nano Mater. 1 (2) (2018) 654–661.

[35] S. Garcia-Segura, E. Vieira dos Santos, C.A. Martínez-Huitle, Role of sp3/sp2 ratio on the electrocatalytic properties of boron-doped diamond electrodes: A mini review, Electrochem. Commun. 59 (2015) 52–55.

[36] T. Watanabe, T.K. Shimizu, Y. Tateyama, Y. Kim, M. Kawai, Y. Einaga, Giant electric double-layer capacitance of heavily boron-doped diamond electrode, Diam. Relat. Mater. 19 (7) (2010) 772–777.

[37] P. Wilczewska, A. Bielicka-Giełdoń, J. Ryl, M. Sobaszek, M. Sawczak, R. Bogdanowicz, K. Szczodrowski, A. Malankowska, F. Qi, E. Maria Siedlecka, Development of novel (BiO)2OHCl/BiOBr enriched with boron doped-carbon nanowalls for photocatalytic cytostatic drug degradation: Assessing photocatalytic process utilization in environmental condition, Appl. Surf. Sci. 586 (2022) 152664.

[38] A. Dettlaff, P. Jakóbczyk, M. Ficek, B. Wilk, M. Szala, J. Wojtas, T. Ossowski, R. Bogdanowicz, Electrochemical determination of nitroaromatic explosives at boron-doped diamond/graphene nanowall electrodes: 2,4,6-trinitrotoluene and 2,4,6-trinitroanisole in liquid effluents, J. Hazard. Mater. 387 (2020) 121672.

[39] A. Medel, E. Bustos, L.M. Apátiga, Y. Meas, Surface Activation of C-sp3 in Boron-Doped Diamond Electrode, Electrocatalysis 4 (4) (2013) 189–195.

[40] R. Trouillon, D. O'Hare, Comparison of glassy carbon and boron doped diamond electrodes: Resistance to biofouling, Electrochim. Acta 55 (22) (2010) 6586–6595.

[41] R.L. McCreery, M.T. McDermott, Comment on Electrochemical Kinetics at Ordered Graphite Electrodes, Anal. Chem. 84 (5) (2012) 2602–2605.

[42] R. Ramesham, Cyclic voltammetric response of boron-doped homoepitaxially grown single crystal and polycrystalline CVD diamond, Sens. Actuators, B 50 (2) (1998) 131–139.

[43] E. Luais, M. Boujtita, A. Gohier, A. Tailleur, S. Casimirius, M.A. Djouadi, A. Granier, P.Y. Tessier, Carbon nanowalls as material for electrochemical transducers, Appl. Phys. Lett. 95 (1) (2009) 014104.

[44] A.G. Krivenko, N.S. Komarova, E.V. Stenina, L.N. Sviridova, K.V. Mironovich, Y.M. Shul'ga, R.A. Manzhos, S.V. Doronin, V.A. Krivchenko, Electrochemical modification of electrodes based on highly oriented carbon nanowalls, Russ. J. Electrochem. 51 (10) (2015) 963–975.

[45] N.S. Komarova, A.G. Krivenko, E.V. Stenina, L.N. Sviridova, K.V. Mironovich, Y.M. Shulga, V.A. Krivchenko, Enhancement of the Carbon Nanowall Film Capacitance. Electron Transfer Kinetics on Functionalized Surfaces, Langmuir 31 (25) (2015) 7129–7137.

[46] A.A. Kava, C.S. Henry, Exploring carbon particle type and plasma treatment to improve electrochemical properties of stencil-printed carbon electrodes, Talanta 221 (2021) 121553.

[47] M. Brycht, S. Baluchová, A. Taylor, V. Mortet, S. Sedláková, L. Klimša, J. Kopeček, K. Schwarzová-Pecková, Comparison of electrochemical performance of various boron-doped diamond electrodes: Dopamine sensing in biomimicking media used for cell cultivation, Bioelectrochemistry 137 (2021) 107646.

[48] M. Raj, P. Gupta, R.N. Goyal, Y.-B. Shim, Graphene/conducting polymer nano-composite loaded screen printed carbon sensor for simultaneous determination of dopamine and 5-hydroxytryptamine, Sens. Actuators, B 239 (2017) 993–1002.

[49] F.J.V. Gomez, A. Martín, M.F. Silva, A. Escarpa, Screen-printed electrodes modified with carbon nanotubes or graphene for simultaneous determination of melatonin and serotonin, Microchim. Acta 182 (11) (2015) 1925–1931.

[50] M. Tertiş, A. Cernat, D. Lacatiş, A. Florea, D. Bogdan, M. Suciu, R. Săndulescu, C. Cristea, Highly selective electrochemical detection of serotonin on polypyrrole and gold nanoparticles-based 3D architecture, Electrochem. Commun. 75 (2017) 43–47.

[51] N.K. Sadanandhan, M. Cheriyathuchenaaramvalli, S.J. Devaki, A.R. Ravindranatha Menon, PEDOT-reduced graphene oxide-silver hybrid nanocomposite modified transducer for the detection of serotonin, J. Electroanal. Chem. 794 (2017) 244–253.

[52] Y. Li, X. Huang, Y. Chen, L. Wang, X. Lin, Simultaneous determination of dopamine and serotonin by use of covalent modification of 5-hydroxytryptophan on glassy carbon electrode, Microchim. Acta 164 (1) (2009) 107–112.

[53] M. Mazloum-Ardakani, A. Khoshroo, High sensitive sensor based on functionalized carbon nanotube/ionic liquid nanocomposite for simultaneous determination of norepinephrine and serotonin, J. Electroanal. Chem. 717–718 (2014) 17–23.

[54] T.D. Thanh, J. Balamurugan, H.V. Hien, N.H. Kim, J.H. Lee, A novel sensitive sensor for serotonin based on high-quality of AuAg nanoalloy encapsulated graphene electrocatalyst, Biosens. Bioelectron. 96 (2017) 186–193.

[55] Y. Wang, S. Wang, L. Tao, Q. Min, J. Xiang, Q. Wang, J. Xie, Y. Yue, S. Wu, X. Li, H. Ding, A disposable electrochemical sensor for simultaneous determination of norepinephrine and serotonin in rat cerebrospinal fluid based on MWNTs-ZnO/chitosan composites modified screen-printed electrode, Biosens. Bioelectron. 65 (2015) 31–38.

[56] S.A. Mozaffari, T. Chang, S.-M. Park, Self-assembled monolayer as a pre-concentrating receptor for selective serotonin sensing, Biosens. Bioelectron. 26 (1) (2010) 74–79.

[57] A.G. Güell, K.E. Meadows, P.R. Unwin, J.V. Macpherson, Trace voltammetric detection of serotonin at carbon electrodes: comparison of glassy carbon, boron doped diamond and carbon nanotube network electrodes, PCCP 12 (34) (2010) 10108–10114.

[58] B.E.K. Swamy, B.J. Venton, Carbon nanotube-modified microelectrodes for simultaneous detection of dopamine and serotonin in vivo, Analyst 132 (9) (2007) 876–884.

[59] A.N. Patel, S.-Y. Tan, T.S. Miller, J.V. Macpherson, P.R. Unwin, Comparison and Reappraisal of Carbon Electrodes for the Voltammetric Detection of Dopamine, Anal. Chem. 85 (24) (2013) 11755–11764.

[60] R. Sainz, M. del Pozo, M. Vilas-Varela, J. Castro-Esteban, M. Pérez Corral, L. Vázquez, E. Blanco, D. Peña, J.A. Martín-Gago, G.J. Ellis, M.D. Petit-Domínguez, C. Quintana, E. Casero, Chemically synthesized chevron-like graphene nanoribbons for electrochemical sensors development: determination of epinephrine, Sci. Rep. 10 (1) (2020) 14614.

[61] B.P. Jackson, S.M. Dietz, R.M. Wightman, Fast-scan cyclic voltammetry of 5-hydroxytryptamine, Anal. Chem. 67 (6) (1995) 1115–1120.

[62] A. Mendoza, T. Asrat, F. Liu, P. Wonnenberg, A.G. Zestos, Carbon Nanotube Yarn Microelectrodes Promote High Temporal Measurements of Serotonin Using Fast Scan Cyclic Voltammetry, Sensors 20 (4) (2020) 1173.